Sensors and Actuators A 267 (2017) 272–277

Contents lists available at ScienceDirect

Sensors and Actuators A: Physical

journal homepage: www.elsevier.com/locate/sna

Birefringence angle sensor for optical displacement measurements

Ruey-Ching Twu*, Nina-Yang Yan

Department of Electro-Optical Engineering, Southern Taiwan University of Science and Technology, No. 1 Nan-Tai Street, Yungkang, Tainan 71005, Taiwan

ARTICLE INFO

Article history:
Received 28 June 2017
Received in revised form 2 October 2017
Accepted 10 October 2017
Available online 13 October 2017

Keywords:
Birefringence
Optical angle sensor
Displacement measurement
Homodyne interferometer

ABSTRACT

A birefringence angle sensor (BAS) was proposed herein for application on a displacement measurement in a homodyne interferometer. The BAS was fabricated using a birefringence plate of potassium titanyl phosphate (KTP) immersed with glycerin liquid in a cylindrical glass container. The lateral displacement of a probe light induces a refractive angle change in the KTP through the curve interface in the glass container. According to the relationship between the displacement and the refracted angle change in the BAS, the measured phase is dependent on the angle change to further obtain actual displacements. Moreover, the flexible incident angles for a tunable sensitivity benefit the displacement measurement range determined by the proposed KTP-BAS.

1. Introduction

Highly precise and widely dynamic linear displacement measurements are important in achieving fine position control in an automatic mechanical system [1]. Therein, non-contact and remote optical measurements have been successfully demonstrated in various applications, including effective vibration analyzers and surface profilers [1–3]. In optical metrology, the physical parameters of measurement may be converted using a prompt transducer. For example, the displacements of probe beams were converted to the propagating angle changes using a lens, a prism or a pair of non-parallel mirrors [4–8]. Next, an optical angle sensor (OAS) may be employed in measuring angle-dependence sensing signals. Finally, the measured signals are used in determining actual displacements by considering the relationship between displacement change and angle variation. Lens type transducers are useful when applied to measurements of transverse and longitudinal displacements where probe lights are perpendicular and parallel to the light paths of the transverse and longitudinal displacements, respectively. When the incident probe light has the transverse displacement on the surface of the lens, the displacement will cause a refractive angle change while passing through the curved interface [5,8]. In addition, the object lens is used as a longitudinal displacement transducer in a con-focal arrangement [2,4,6]. The reflection mirror is placed at a focal point of the object lens. Therein, the probe light passes through the lens and is then reflected from the movable mirror; an angle change of the reflected light is dependent upon the displacement between the object lens and the mirror.

In recent decades, the OASs have been widely demonstrated according to the principles of surface plasmon resonance (SPR) and total internal reflection (TIR) [4–6]. In the SPR-OAS, there is an essential change in both the intensity and phase signals at a resonance angle. High sensitivity with the stepper phase change is achievable. Therefore, phase-interrogation with high resolution has been evaluated for angle measurements in a common-path heterodyne interferometer [4]. The phase modulating schemes are well known techniques to be applied in the phase-interrogation interferometers. Especially, the sinusoidal and sawtooth phase modulations are adopted for the homodyne and heterodyne interferometers, respectively [4,14]. In the case of the TIR-OAS, an abrupt change in intensity occurred at a critical angle under the TIR condition [6]. The intensity-interrogation was achieved by receiving the voltage signal based on differential amplification operations. To extend the dynamic range, phase-interrogation TIR-OAS was studied when the incident angle of the probe light was over the critical angle [5]. The SPR-based displacement measurements are able to achieve the highest resolution as compared to TIR measurements. However, limited displacement range and a specific resonance angle are the main drawbacks. Moreover, the sensitivity of SPR is critically dependent on a specific film thickness and a dielectric constant of the coated gold film, both of which rely on a stable fabrication process [9,10]. Moreover, it is also necessary to start at the resonance angle by using the precise rotational stage with an angular resolution of 0.001° [8].

In this study, a birefringence angle sensor (BAS) was proposed for application to a displacement measurement in a dual-channel

* Corresponding author.
E-mail address: rctwu@stust.edu.tw (R.-C. Twu).

https://doi.org/10.1016/j.sna.2017.10.027
0924-4247/

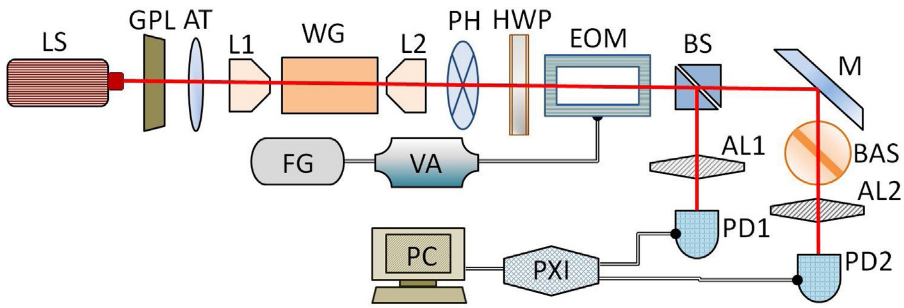

(a)

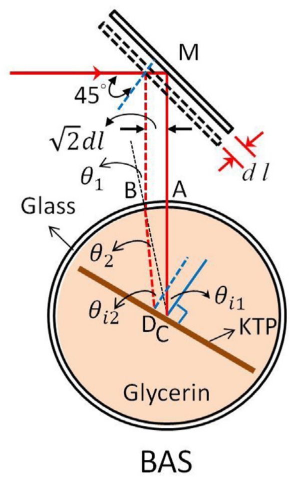

(b)

Fig. 1. (a) Measurement setup. (b) Schematic drawing for the displacement and refraction of the sensing light in the BAS.

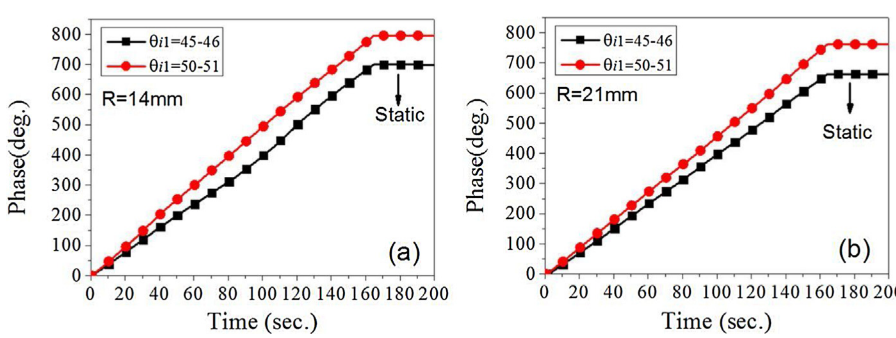

Fig. 2. Phase variation versus angle scanning time for different radiuses of BAS: (a) R = 14 mm and (b) R = 21 mm.

homodyne interferometer. Typically, the birefringent materials can induce a phase delay between two orthogonal polarizations of a propagating light that are widely used for fabricating wave plates and liquid crystal modulators [11,12]. The phase delay is dependent on birefringence and the thickness of the birefringent plate as well as an incident light angle [11]. Moreover, the relative refractive index between the birefringent plate and the environment will also alter the phase delay values. The principle and fabrication of the BAS have been systematically evaluated in our previous study [13]. To extend the application, the BAS was used further as the displacement transducer in a dual-channel homodyne interferometer [14]. The different sizes of BAS were evaluated to explore measurement performance. In comparison with the SPR- and TIR-OASs [4,5], the proposed BAS has the advantages of a flexible incident angle and a wide linear dynamic range for displacement measurements.

2. BAS for displacement measurements

Fig. 1 illustrates the measurement setup for the optical displacement measurement utilizing the BAS in a dual-channel homodyne interferometer. A linearly polarized He-Ne laser of 632.8 nm wavelength (LS) was launched through a Glan-Thompson (GPL) with an extremely high extinction ratio of 10^6. The optical power was tuned using an absorption-type attenuator (AT). The light was coupled by lens (L1) into a Zn-indiffused lithium niobate channel waveguide (WG). To fabricate a single-mode waveguide, a 35 nm Zn film with a predeposition Ni film of 5 nm was deposited over the substrate via e-beam evaporation. Then, the waveguide width of 4 μm was formed by a lift-off technique. After thermal diffusion of 850 °C for 120 min, the substrate end faces were polished for the light coupling. The output light from the WG was focused by another lens

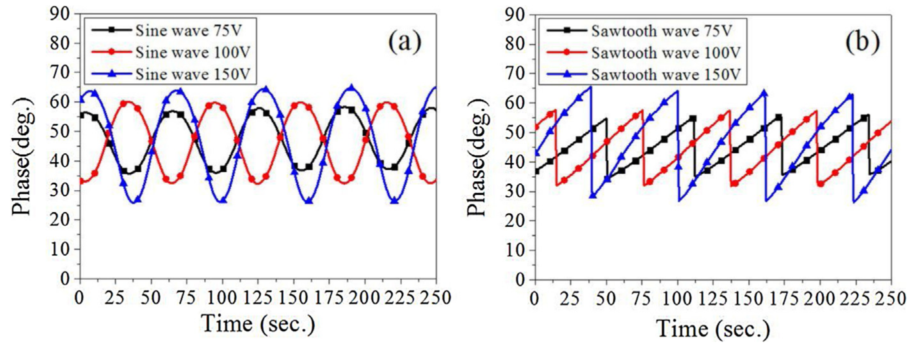

Fig. 3. Phase variations under different applied waveforms and voltages for the BAS with radius 14 mm and an incident angle of 45°: (a) sinusoidal voltage and (b) sawtooth voltage.

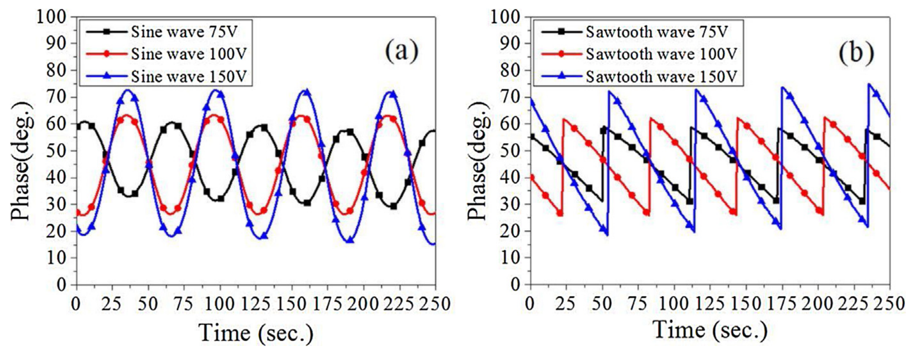

Fig. 4. Phase variations under different applied waveforms and voltages for the BAS with radius 14 mm and an incident angle of 50°: (a) sinusoidal voltage and (b) sawtooth voltage.

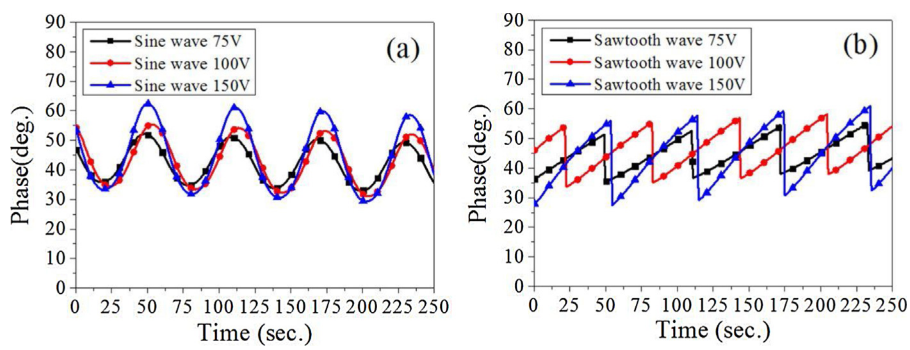

Fig. 5. Phase variations under different applied waveforms and voltages for the BAS with radius 21 mm and an incident angle of 45°: (a) sinusoidal voltage and (b) sawtooth voltage.

(L2) to narrow the probe beam size with low divergence in the measurement. The scattering light was blocked through a pin hole (PH). A half-wave plate (HWP) at azimuth angle of 22.5° was used to provide the probe light with equally orthogonal polarizations (TE-wave and TM-wave polarizations) in the polarimetric interferometer. Phase modulation light was generated by the application of sinusoidal voltage onto an electro-optical modulator (EOM) driven by a function generator (FG) and a voltage amplifier (VA). Although the input probe light is a 45° linear polarization with respect to a horizontal axis of laboratory coordinate. The state of polarization of the probe light was modulated periodically after the EOM. The applied voltage and driving frequency were 105 V and 1 kHz, respectively. The probe light was divided into two different paths by a beam splitter (BS). The transmitted and reflected paths are used as a sensing and a reference light, respectively. The transmitted light is incident on a mirror (M), which was placed on a motional stage. Then, the reflected light passed through the BAS. The BAS was placed on the center of a rotational motion stage (RMS). The initial incident angles were adjustable by the RMS. In this BAS, a 1 mm thick birefringence plate of potassium titanyl phosphate (KTP, a biaxial crystal for three different refractive indices [13]) was immersed in a cylindrical glass container filled with a glycerin liquid with a refractive index of 1.473. Next, two analyzers AL1 and AL2 were oriented at 45° with respect to a horizontal axis of laboratory coordinate, and both interferometric signals detected by PD1 and PD2 were connected to a multichannel data acquisition module (PXI) and a personal computer (PC). The two interferometric signals P_1 and P_2 from the PD1 and PD2 are represented by:

$$P_1 = I_{TE} + I_{TM} + 2\sqrt{I_{TE} \cdot I_{TM}} \cdot \cos(\gamma \cdot \sin(2\pi ft) + \phi_{PN}) \quad (1.a)$$

$$P_2 = I_{TE} + I_{TM} + 2\sqrt{I_{TE} \cdot I_{TM}} \cdot \cos(\gamma \cdot \sin(2\pi ft) + \phi_{BAS} + \phi_{PN}), \quad (1.b)$$

where I_{TE} and I_{TM} are the intensities of the TE-wave and TM-wave polarizations, respectively; ϕ_{PN} is the phase noise mainly induced from the photorefractive effects of the EOM; ϕ_{BAS} is the phase signal from the BAS; and γ and f are the modulation depth and frequency of the applied voltage for the phase modulation, respectively. γ is defined as:

$$\gamma = \pi \cdot \frac{V_{ac}}{V_{\pi}}, \tag{2}$$

where V_{ac} and V_{π} are the applied voltage and voltage for the phase change of π, respectively.

The measured signal was processed utilizing a Fast Fourier Transform (FFT) scheme. The spectrum with different harmonic signals can be used to calculate phase information in the LabVIEW-based dual-channel instrument as reported in [14]. In case of the reference signal from the PD1, the components of the fundamental and second harmonic frequencies (I_{ref_1f} and I_{ref_2f}) are represented by:

$$I_{ref\_1f} = 4\sqrt{I_{TE} \cdot I_{TM}} \cdot \sin\left(\phi_{ref}\right) \cdot J_{ref\_1}(\gamma) \tag{3.a}$$

$$I_{ref\_2f} = 4\sqrt{I_{TE} \cdot I_{TM}} \cdot \cos\left(\phi_{ref}\right) \cdot J_{ref_2}(\gamma), \tag{3.b}$$

where $J_{ref\_1}(\gamma)$ and $J_{ref\_2}(\gamma)$ are the first kind of Bessel function with different indices. According to Eqs. (3.a) and (3.b), the measured phase of the reference signal can be defined as:

$$\phi_{ref} = \phi_{PN} = tan^{-1}\left(\frac{I_{ref\_1f} \cdot J_{ref\_2}(\gamma)}{I_{ref\_2f} \cdot J_{ref\_1}(\gamma)}\right). \tag{4}$$

Similarly, the measured phase of the sensing signal PD2 can be defined as:

$$\phi_{sen} = \phi_{BAS} + \phi_{PN} = tan^{-1}\left(\frac{I_{sen\_1f} \cdot J_{sen\_2}(\gamma)}{I_{sen\_2f} \cdot J_{sen\_1}(\gamma)}\right). \tag{5}$$

The common phase noise ϕ_{PN} can be cancelled by subtracting between Eqs. (4) and (5). The measured phase amplitudes from the BAS were obtained by $\phi_{BAS} = \phi_{sen} - \phi_{ref}$.

The principle of displacement measurement employing the BAS is shown schematically in Fig. 1(b). The axial displacement of the mirror dl will result in a lateral displacement $\sqrt{2}dl$ of the sensing light at an incident angle of 45°. The sensing light passes through center C of the KTP plate in the BAS. The sensing light transmits through A and C at the initial positions. The RMS is able to adjust the initial incident angle $\theta_{i1}$of the BAS. After the lateral shift, the position of the sensing light is changed from A to B. The refracted light from B to D has the incident angle θ_{i2}. There is an angle difference (θ_1)between the two normal lines AC and BC since the radius R (~mm) of the cylindrical cell is around 1000 times larger than the lateral shift dl (~μm). The θ_1 is approached as $\sqrt{2}dl/R$.The shifted sensing light is refracted through the liquid in the glass container. The refracted angle in respect to the line BC is defined as θ_2. The glass container is an intermediate layer between the incident space (n_a) and the immersed liquid (n_l), where n_a and n_l are the refractive indices for the air and liquid, respectively. The relationship between θ_1 and θ_2 is expressed as $n_a sin\theta_1 = n_l sin\theta_2$. At the small θ_1, the θ_2 is approached by $\theta_2 = \frac{n_a}{n_l} \cdot \theta_1$. Since the lateral displacement induces the incident angle, it is changed from θ_{i1} to θ_{i2}. The difference between the incident angles is given by $d\theta = \theta_{i2} - \theta_{i1}$, and also can be represented by:

$$d\theta = \theta_1 - \theta_2 = \left(\frac{n_l - n_a}{n_l}\right) \cdot \theta_1. \tag{6}$$

In this KTP-BAS, the phase delay ϕ_{BAS} between two orthogonal polarizations is dependent on the incident angleand relative refractive index, as discussed in a previous study [13]. The amplification factor AF of the BAS is represented by:

$$AF = \frac{d\phi_{BAS}}{d\theta} = \frac{2\pi}{\lambda} \cdot t \cdot n_l^2 \cdot sin\theta_{i1} \cdot cos\theta_{i1} \cdot \left[\frac{1}{\sqrt{n_y^2 - n_l^2 \cdot \left(\frac{n_y^2}{n_x^2}\right) \cdot sin^2\theta_{i1}}} - \frac{1}{\sqrt{n_z^2 - n_l^2 \cdot sin^2\theta_{i1}}}\right], \tag{7}$$

where λ and t are the measurement wavelength and thickness of the KTP plate, respectively. Three different refractive indices for the KTP plate are n_x, n_y, and n_z [13]. At the same BAS, the AF is adjustable according to the θ_{i1} by controlling the RMS. The relationship between the measured phase variation $d\phi_{BAS}$ and the displacement change dl is defined as:

$$d\phi_{BAS} = AF \cdot \left(\frac{n_l - n_a}{n_l}\right) \cdot \frac{\sqrt{2}dl}{R}. \tag{8}$$

The displacement measurement sensitivity (DMS) of the measurement system is expressed by:

$$DMS = \frac{d\phi}{dl} = \frac{\sqrt{2} \cdot AF}{R} \cdot \left(\frac{n_l - n_a}{n_l}\right). \tag{9}$$

As defined in Eq. (7), the AF is a key item to reflect the relation between the measured phase amplitude and the incident angle variation. It can provide the designed parameters of the BAS including the birefringent plate, refractive index of liquid, and radius of the container. Moreover, the relation between the AF and the incident angle can optimize the initial incident angle for the measurements [13]. According to Eq. (9), the DMS is proportional to the AF. The higher AF can enhance the DMS and improve a measurement resolution of the displacement.

3. Experimental results

The BASs with different radii were placed on the center of the RMS. The average scanning rate of angular displacement was around 6×10^{-3}°/sec. In a low and constant speed rotation, the angular displacement is linearly changed, and the relation between the displacement and time is linearity. Therefore, the relation between the phase and time is also linearity in the small angle scanned range. According to Eq. (7), the AF is simply defined as a slope of the phase curve. The calculated AF was obtained after doing a linear fit of the phase curve as shown in Fig. 2. In case of R = 14 mm, the phase variation versus angle scanning time is shown in Fig. 2(a); the values of AF are around 700 and 796 for the initial incident angles 45° and 50° with the same angular displacement of 1°. With the same angle scanning conditions, Fig. 2(b) indicates the values of AF are around 663 and 762 for the R = 21 mm. It was found that the larger incident angle can obtain the higher AF; the same tendency was reported in [13]. At the same incident angles, the values of AF show only a slight difference for the different radii of BAS.

Fig. 3 expresses the displacement-induced phase variations for the R = 14 mm at an incident angle of 45°. The phase amplitudes are 21.2, 27.5, and 38.4 deg for the applied sinusoidal voltages of 75, 100, and 150 V, respectively, as shown in Fig. 3(a). Fig. 3(b) indicates that the phase amplitudes are 20.4, 25.6, and 36.7 deg for the applied sawtooth voltages of 75, 100, and 150 V, respectively.

To increase measurement sensitivity, the incident angle was increased to 50°; the phase measurements are shown in Fig. 4. The phase amplitudes are 28.8, 36.7, and 55.1 deg for the applied sinusoidal voltages of 75, 100, and 150 V, respectively, as shown in Fig. 4(a). Fig. 4(b) shows that the phase amplitudes are 27.4, 36.3, and 53.3 deg for the applied sawtooth voltages of 75, 100, and 150 V, respectively. According to Figs. 3 and 4, the peak values of phase change for different applied voltages are similar for the sinusoidal and sawtooth signals. The measurement results also represent good repeatability for the two radii of BAS.

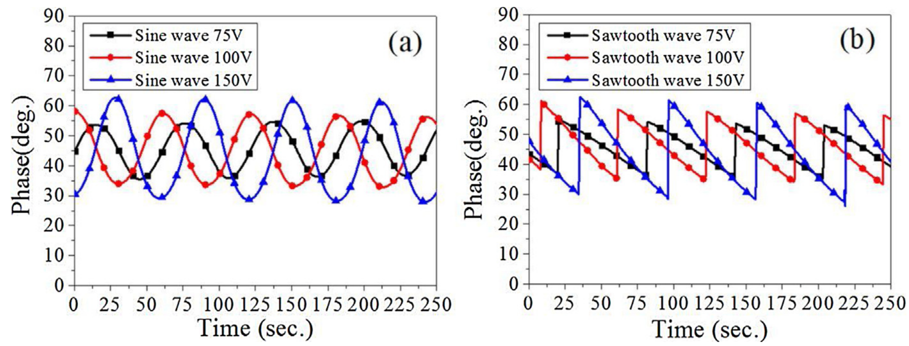

Fig. 6. Phase variations under different applied waveforms and voltages for the BAS with radius 21 mm and an incident angle of 50°: (a) sinusoidal voltage and (b) sawtooth voltage.

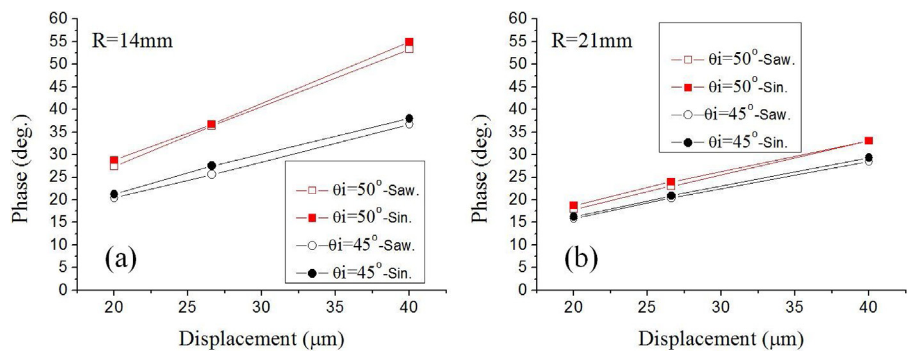

Fig. 7. Phase variation versus displacement for the different radiuses and incident angles: (a) R = 14 mm and (b) R = 21 mm.

Fig. 5 gives the measurement results of the R = 21 mm at an incident angle of 45°. Fig. 5(a) shows the phase amplitudes are 16.3, 20.9, and 29.3 deg for the applied sinusoidal voltages of 75, 100, and 150 V, respectively. Fig. 5(b) shows the phase amplitudes are 15.9, 20.4, and 28.5 deg for the applied sawtooth voltages of 75, 100, and 150 V, respectively.

Fig. 6 represents the measurement results of the R=21 mm at an incident angle of 50°. Fig. 6(a) shows the phase amplitudes are 18.7, 24.1, and 33.2 deg for the applied sinusoidal voltages of 75, 100, and 150 V, respectively. Fig. 6(b) shows the phase amplitudes are 17.9, 23.5, and 33.1 deg for the applied sawtooth voltages of 75, 100, and 150 V, respectively.

The relation between the phase amplitude $d\phi_{BAS}$ and the displacement dl is generally given by Eq. (8). There is a good linearity between them when the AF is a constant value under the small displacement. As shown in Figs. 3–6, the time-dependent phase curves are represented for the displacement changes by applying the different sinusoidal and sawtooth voltages on the motional stage. Therefore, the phase curves are similar to the applied voltage waveforms.

According to the product specifics from the vender, displacement is around 40 μm at the applied voltage of 150 V in the motional stage (Thorlabs Max 312D/M). The summarized phase variations versus displacements for the BAS with the radii of 14 mm and 21 mm are shown in Fig. 7(a) and (b), respectively. The average DMS is calculated by considering the slope between phase variation and displacement by a linear fit. Fig. 7(a) gives the average values of 0.84 and 1.31 deg/μm for the incident angles 45° and 50°, respectively. Fig. 7(b) shows the average values are 0.64 and 0.74 deg/μm for the incident angles 45° and 50°, respectively. According to Eq. (4), the DMS is proportional and inversely proportional to AF and R, respectively. At the same R, the larger incident angle with higher AF can enhance the DMS since the difference of AF is slight for the different radius of BAS at the same incident angles. In principle, the DMS is increased by using the smaller radius of BAS. However, the larger curvature in the smaller radius easily induces a lens-like aberration to reduce measurement linearity. In our experiments, the linearity is worse at a radius smaller than 14 mm. If the beam size of the sensing light can be further narrowed, it should be possible to use a smaller glass container. From the experimental data measured in a static period as shown in Fig. 2, the average standard deviation is calculated to be 0.11 deg and the best DMS is 1.31 deg/μm. Under these conditions, the available minimum displacement of 84 nm is achievable.

4. Conclusions

A simple and novel transmitted-type KTP-BAS has been successful in measuring a small displacement in a homodyne interferometer. The dual-channel phase measurements can reduce the phase errors from the photorefractive effect in the EOM. According to the experimental data, the average standard deviation is 0.11 deg and the best DMS is 1.31 deg/μm. The available minimum displacement of 84 nm is achievable in a displacement range of at least 40 μm. The results show that the proposed BAS has advantages of a flexible incident angle and a wide displacement range.

Acknowledgement

This study was supported in part by the Ministry of Science and Technology in Taiwan under grant number MOST 105-2221-E-218-014.

References

[1] X. Li, W. Gao, H. Muto, Y. Shimizu, S. Ito, S. Dian, A six-degree-of-freedom surface encoder for precision positioning of a planar motion stage, Precision Eng. 37 (2013) 771–781.

[2] D.J. Park, G.J. Park, T.S. Aum, J.H. Yi, J.H. Kwon, Measurement of displacement and vibration by using the oblique ray method, Appl. Opt. 45 (2006) 3728–3732.
[3] G. Jäger, T. Hausotte, E. Manske, H.-J. Büchner, R. Mastylo, N. Dorozhovets, N. Hofmann, Nanomeasuring and nanopositioning engineering, Measurement 43 (2010) 1099–1105.
[4] M.H. Chiu, B.Y. Shih, C.W. Lai, L.H. Shyua, T.H. Wu, Small absolute distance measurement with nanometer resolution using geometrical optics principles and a SPR angular sensor, Sens. Actuators A: Phys. 141 (2008) 217–223.
[5] K.H. Chen, H.S. Chiu, J.H. Chen, Y.C. Chen, An alternative method for measuring small displacements with differential phase difference of dual-prism and heterodyne interferometry, Measurement 45 (2012) 1510–1514.
[6] Y. Ku, C. Kuang, D. Luo, T. Wang, H. Li, Differential internal multi-reflection method for nano-displacement measurement, Opt. Lasers Eng. 50 (2012) 1445–1449.
[7] M.H. Chiu, W.C. Chen, C.T. Tan, Small displacement measurements based on an angular-deviation amplifier and interferometric phase detection, Appl. Opt. 54 (2015) 2885–2890.
[8] J.Y. Lin, K.H. Chen, J.H. Chen, Measurement of small displacement based on surface plasmon resonance heterodyne interferometry, Opt. Lasers Eng. 49 (2011) 811–815.
[9] B. Ran, S.G. Lipson, Comparison between sensitivities of phase and intensity detection in surface plasmon resonance, Opt. Express 14 (2006) 5641–5650.
[10] J.Y. Lee, S.K. Tsai, Measurement of refractive index variation of liquids by surface plasmon resonance and wavelength-modulated heterodyne interferometry, Opt. Comm. 284 (2011) 925–929.
[11] C.H. Hsieh, C.C. Tsai, H.C. Wei, L.P. Yu, J.S. Wu, C. Chou, Determination of retardation parameters of multiple-order wave plate using a phase-sensitive heterodyne ellipsometer, Appl. Opt. 46 (2007) 5944–5950.
[12] J. Yan, M. Jiao, L. Rao, S.T. Wu, Direct measurement of electric-field-induced birefringence in a polymer-stabilized blue-phase liquid crystal composite, Opt. Express 18 (2010) 11450–11455.
[13] R.C. Twu, C.S. Wang, Birefringent-refraction transducer for measuring angular displacement based on heterodyne interferometry, Appl. Sci. 6 (2016) 208.
[14] R.C. Twu, H.Y. Hong, H.H. Lee, Dual-channel optical phase measurement system for improved precision, Opt. Lett. 33 (2008) 2530–2532.

Biographies

Ruey-Ching Twu received the Ph.D. degree in Graduate Institute of Electro-Optical Engineering (2000) from National Taiwan University, Taiwan. He is currently a professor at Southern Taiwan University of Science and Technology, Department of Electro-Optical Engineering. His research interests include integrated optics, optical metrology systems, and sensors.

Nina-Yang Yan received his M.Sc. degree in Department of Electro-Optical Engineering (2016) from Southern Taiwan University of Science and Technology, Taiwan. His research interests include optical instrument designs, and optical sensor developments.